

A Numerical Model for Periodic Finite Amplitude Waves on a Rotational Fluid

ROBERT A. DALRYMPLE

*Department of Civil Engineering, College of Engineering and the College of Marine Studies,
University of Delaware, Newark, Delaware 19711*

Received June 10, 1976; revised September 22, 1976

An iterative finite difference model is developed to describe two-dimensional periodic gravity waves on the surface of a fluid containing vorticity in the form of a vertical shear current. A coordinate transformation due to Dubreil-Jacotin has been used to map the fluid domain into a rectangle. The full nonlinear constant pressure free surface boundary condition is used iteratively until convergence is achieved. A comparison is made to an analytical model for a linear shear current and results are also shown for a mean flow with a $(\frac{1}{2})$ power law velocity distribution.

INTRODUCTION

Gravity waves propagating on the surface of a fluid have been the impetus for numerous analytical and numerical studies since the 1800s. The goal has been to describe the fluid particle kinematics and the free surface displacements due to the presence of the waves. Few studies, however, have allowed the inclusion of currents, other than those induced by the waves; yet, in nature, currents are almost always present, modifying the wave characteristics.

Early studies, such as those by Airy [1] and Stokes [2], were concerned with irrotational water waves on an incompressible and inviscid fluid. To this day, the Stokes wave theory, which has been carried out to high orders in wave steepness analytically [3], is used for offshore design. Gerstner [4] developed the first exact finite amplitude rotational water wave theory, yet his theory is incapable of allowing a mean flow, further, the sense of the fluid vorticity of the fluid particles is in the opposite direction of the orbital motion induced by the waves.

Numerical solutions to water wave problems have been obtained many ways. Numerical perturbation procedures using the velocity potential [5] and the stream function [6] for finite amplitude irrotational water waves can be used to any arbitrary order. Dalrymple [7] has extended Dean's [6] stream function approach to waves on linear shear currents. Dalrymple and Cox [8] have used a similar method for shear current profiles which vary exponentially over depth. From purely numerical approaches the time-dependent wave motion of a fluid has been studied by Hirt *et al.* [9], Nichols and Hirt [10], including the effects of fluid viscosity, and by Chan and

Street [11], using a modified marker and cell approach for a solitary wave on an ideal fluid. None of these procedures include a current.

Recently, Chan [12] examined solitary waves utilizing a transformed coordinate system and the full nonlinear free surface boundary condition (constant pressure). His iterative technique at the free surface is similar to the one used here. The analytical analog to his study for periodic waves was developed by von Schwind and Reid [13]. Again, these studies are conducted for an ideal, or irrotational, fluid.

Mme. Dubreil-Jacotin [14], extending the convergence proofs of Levi-Civita [15] and Struick [16] for irrotational waves to waves on arbitrary vorticity distributions and thus arbitrary current velocity profiles over depth, used a variable transformation. Her technique was later applied to periodic waves via a perturbation approach by Daubert [17] and by Brooke-Benjamin [18] to solitary waves. The Dubreil-Jacotin transformation was used here to develop a finite difference model for finite amplitude propagation of a fluid possessing an arbitrary vorticity distribution.

The model describes periodic waves, as these are most useful for offshore design, however, it can be adapted to treat solitary waves by a modification of the lateral boundary conditions (cf. [18]).

GOVERNING EQUATIONS

Assuming a two-dimensional incompressible fluid overlaying an impermeable horizontal bottom, a stream function exists and can be used to describe the water particle motions by the following definitions.

$$\begin{aligned} U + u - C &= -\psi_y, \\ v &= \psi_x. \end{aligned} \tag{1}$$

Here (U, u, v) refer to the mean current velocity and the horizontal and vertical wave-induced velocities and C is the phase speed of the wave, unknown a priori. The problem has been rendered steady state by translating the coordinate system with the wave speed. The fluid vorticity is given by Lamb [19],

$$\psi_{xx} + \psi_{yy} = f(\psi) \tag{2}$$

where $f(\psi)$ is constant on a streamline and is the vorticity distribution function. For the classical wave theories of Airy and Stokes, $f(\psi) = 0$. The difficulty with this problem lies in the fact that $f(\psi)$ is a function of the dependent variable, $\psi(x, y)$ and that a priori the domain of the fluid is unknown as the surface displacement, $y = \eta(x)$, is unknown.

To eliminate these difficulties, Dubreil-Jacotin developed a coordinate transformation which maps the wave domain into a rectangle and fixes the free surface, by posing the problem with y as a function of x and ψ . Her transformation results by using the stream function definitions, Eq. (1), written as

$$U + u - C = -(1/y_\psi); \quad v = -(y_x/y_\psi) \tag{3}$$

and transforming Eq. (2). The resulting nonlinear second-order equation is

$$y_{\psi}^2 y_{xx} - 2y_x y_{\psi} y_{x\psi} + (1 + y_x^2) y_{\psi\psi} = -y_{\psi}^3 f(\psi). \tag{4}$$

Despite the obviously more difficult governing equation, the domain of the problem has been transformed into a rectangle, with a base the length of the wave and a height equal to the value of the surface streamline, ψ_n , rather than the wave-shaped region for the Poisson equation (Eq. (2)). See Fig. 1, noting that due to symmetry only one-half the length of the wave need be studied. In the transformed domain, y refers to the elevation above the bottom.

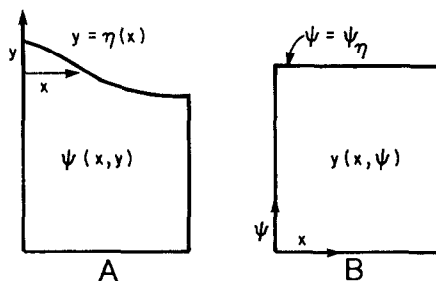


FIG. 1. Fluid domains for rotational water waves (a) Conventional stream function approach. (b) Dubreil-Jacotin transformed coordinates.

A further advantage is gained as the vorticity distribution, $f(\psi)$, is now specified as a function of an independent variable. Dubreil-Jacotin showed that for a given wave number, k , water depth, h , a wave height parameter, and an $f(\psi)$, there is a rotational wave which exists and is unique. Dubreil-Jacotin did not, however, offer a solution to her equation.

The boundary conditions to be satisfied by the governing equations are that there be no flow through the bottom, the solution be periodic in the direction of propagation, taken to be the x -coordinate direction, and that the free surface be a constant pressure streamline. It is only the last of these that proves to be a problem, due to the nonlinearities involved. The computational technique will involve using the Bernoulli equation along the free surface streamline in an iterative method to achieve the final solution.

FINITE DIFFERENCE FORMULATION

In order to readily adapt the Dubreil-Jacotin equation to finite difference form, it is convenient to cast the problem into dimensionless form by defining the following dimensionless variables.

$$y' = \frac{y}{h}; \quad x' = kx; \quad \psi' = \frac{\psi}{\psi_n}; \quad f'(\psi) = \frac{f(\psi) h^2}{\psi_n} \tag{5}$$

where h is the still water depth, k ($= 2\pi/L$) is the wave number, and ψ_η is the value of the surface streamline. Therefore, the governing equation may be written in non-dimensional form. The primes have been omitted for convenience for the remainder of the paper and Eq. (4) takes the form

$$-\frac{y_\psi^3}{(kh)^2} f(\psi) = y_{xx} y_\psi^2 - 2y_{x\psi} y_x y_\psi + y_{\psi\psi} \left[\frac{1}{(kh)^2} + y_x^2 \right]. \tag{6}$$

The rectangular domain of the solution must be represented by a grid, which extends from 0 to π in the x direction and from 0 to 1 in the ψ coordinate direction. Figure 2 is a schematic of the grid system; the i index refers to the ψ direction and the j index, the x direction. The requirement that the solution is periodic in x necessitates the inclusion of two extra columns of grid points, at $x = -\Delta x$ and at $x = \pi + \Delta x$, as will be discussed shortly.

By use of central differences, differential equation (6) may be approximated by

$$v(j, i) = \frac{\left[-y_{x\psi} y_x y_\psi + \left[\frac{y(j-1, i) + y(j+1, i)}{2} \right] \frac{y_\psi^2}{(\Delta x)^2} + \left[\frac{y(j, i+1) + y(j, i-1)}{2} \right] \frac{\left(\frac{1}{(kh)^2} + y_x^2 \right)}{(\Delta \psi)^2} + \frac{f(i) y_\psi^3}{2(kh)^2} \right]}{\frac{y_\psi^2}{(\Delta x)^2} + \frac{\left(\frac{1}{(kh)^2} + y_x^2 \right)}{(\Delta \psi)^2}} \tag{7}$$

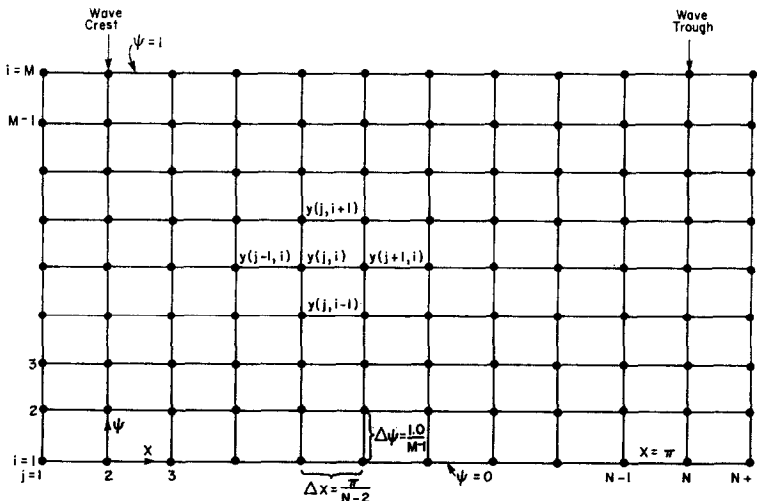


FIG. 2. Schematic of the finite difference scheme utilized for the Dubreil-Jacotin equation.

where

$$y_x = \frac{y(j+1, i) - y(j-1, i)}{2\Delta x}; \quad y_\psi = \frac{y(j, i+1) - y(j, i-1)}{2\Delta\psi},$$

$$y_{x\psi} = \frac{y(j+1, i+1) - y(j-1, i+1) + y(j-1, i-1) - y(j+1, i-1)}{4\Delta x \Delta\psi}$$

and $f(i)$ is a discrete representation of $f(\psi)$. As with all elliptic equations, Eq. (7) shows that $y(j, i)$ is a weighted average of its neighboring points.

The boundary condition at the bottom is satisfied by specifying $y(j, 1) = 0$ (for $1 \leq j \leq N + 1$), thus the vertical velocity $v (= -y_x/y_\psi)$ is zero at the bottom. The periodicity requirement is imposed by specifying $y(1, i) = y(3, i)$ and $y(N + 1, i) = y(N - 1, i)$ (for $1 \leq i \leq M$) which reflects y about the wave crest and trough.

The more difficult boundary conditions are those at the surface. These are the mean sea level constraints, which insures that the presence of the wave does not alter the mean free surface location, the dynamic free surface boundary condition (DFSBC), and the wave height constraint, which assures that the model converges to a given wave height. The first is written, in dimensionless form as

$$(1/\pi) \int_0^\pi y(j, M) dx = 1 \quad \text{on} \quad \psi = 1, \text{ the surface streamline.}$$

In finite difference form, Simpson's rule is used to carry out the integration and this integration will be denoted hereafter as

$$S[y(j, M)] \equiv (\Delta x/3\pi)[y(2, M) + 4y(3, M) + 2y(4, M) + \dots + 2y(N - 2, M) + 4y(N - 1, M) + y(N, M)].$$

The DFSBC which forces the pressure to be constant along the free surface is imposed by specifying that the Bernoulli constant $Q(j)$ be equal to \bar{Q} at all grid points on the free surface streamline, which in dimensionless form is

$$Q(j) = y(j, M) + \frac{\psi_\eta^2}{2gh^3} \frac{[1 + (khy_x)^2]}{y_\psi^2} = \bar{Q} \quad \text{for all } j (i = M) \quad (8)$$

where

$$\bar{Q} = \frac{1}{(N-1)} \sum_{j=2}^N Q(j)$$

and g is the acceleration of gravity.

SOLUTION TECHNIQUE

The finite difference solution is obtained iteratively due to nonlinearities inherent in the free surface boundary condition. First, an approximate solution is used to

initialize the $y(j, i)$. This approximate solution for a wave of height, H , may be the first-order Daubert [17] solution in dimensionless form

$$y(x, \psi) = \psi + \frac{H \sinh\left(\frac{k\psi_n\psi}{C}\right)}{2h \sinh\left(\frac{k\psi_n}{C}\right)} \cos x \quad (9a)$$

or

$$y(x, \psi) = \psi + \frac{H \sinh kh\psi}{2h \sinh kh} \cos x \quad (9b)$$

(as to first order, $\psi_n = Ch$) or the numerical shear current solution of Dalrymple [7]. Next, the finite difference form of governing equation (7) is used to improve the fit of the interior points to the equation. The method of applying the equation to the grid used here is successive overrelaxation or the SOR method. It was experimentally found that for a relaxation parameter of $\theta_0 = 1.73$, there is a large reduction of the numbers of sweeps over the grid necessary for convergence. (This value of θ_0 is also the optimum value for the solution of the Laplace equation, Roache [20].) In comparison to the Leibmann method, there was an eightfold reduction in the number of sweeps for convergence. In practice, as the final solution was approached, the θ_0 parameter was reduced to achieve monotonic convergence.

After a number of sweeps (e.g., 15 to 20), the errors to the free surface boundary conditions are then evaluated. The free surface, $y(j, M)$ is evaluated, using a backward difference form of governing equation (6). This ensures that the vorticity at the surface, $f(M)$, is included into the DFSBC. The errors in the DFSBC are defined in terms of an objective function given as

$$O^k = \frac{1}{(N-1)} \sum_{j=2}^N [Q(j) - \bar{Q}]^2 + \lambda_1[S[y(j, M)] - 1] + \lambda_2[y(2, M) - y(N, M) - H] \quad (10)$$

and was used by Dalrymple [7]. An exact solution will yield O^k equal to zero and, therefore, the solution procedure seeks to minimize O^k .

The first term of O^k is defined here as the DFSBC error and its magnitude is used as an indicator of convergence. From Eq. (8) it is evident that $Q(j)$ is a function of $y(j-1, M)$, $y(j, M)$, and $y(j+1, M)$ and, therefore, the value of O^{k+1} may be approximated by a first-order Taylor series in $y(j, M)^k$, where k refers to the iteration.

$$\begin{aligned} O^{k+1} = & \frac{1}{(N-1)} \sum_{j=2}^N [Q(j)^k - \bar{Q}^k]^2 + \frac{1}{(N-1)} \sum_{l=2}^N \sum_{j=2}^N [Q(j)^k - \bar{Q}^k]_{y(l, M)} y'(l, M) \\ & + \lambda_1[S[y(j, M) + y'(j, M)] - 1] \\ & + \lambda_2[y(2, M) + y'(2, M) - y(N, M) - y'(N, M) - H] \end{aligned} \quad (11)$$

where the subscript indicates partial differentiation and $y'(l, M)$ indicates a small correction to $y(l, M)$. Minimizing O^{k+1} with respect to $y'(n, M)$ and retaining only first-order derivatives gives the equations

$$\begin{aligned} (O^{k+1})_{y(n, M)} &= \frac{2}{(N-1)} \sum_{j=2}^N [Q(j)^k - \bar{Q}^k][Q(j)^k - \bar{Q}^k]_{y(n, M)} \\ &+ \sum_{l=2}^N [Q(j)^k - \bar{Q}^k]_{y(n, M)} [Q(j)^k - \bar{Q}^k]_{y(l, M)} y'(l, M) \\ &+ \frac{\lambda_1 \Delta x}{3\pi} \begin{cases} 1, & n = 2, N \\ 4, & n \text{ even} \\ 2, & n \text{ odd} \end{cases} + \lambda_2 \begin{cases} 1, & n = 2, N \\ 0, & n \neq 2, N \end{cases} = 0. \end{aligned} \quad (12)$$

By letting $n = 2$ through N , $N - 1$ equations result for the $N + 1$ unknowns, $y'(j, M)$, λ_1 and λ_2 . By minimizing O^{k+1} with respect to the λ_1 , two further equations result.

$$\begin{aligned} S[y'(j, M)] &= 1.0 - S[y(j, M)], \\ y'(2, M) - y'(N, M) &= H - [y(2, M) - y(N, M)]. \end{aligned} \quad (13)$$

There are now $N + 1$ equations which may be solved by matrix methods for the $y'(j, M)$ which are then added to the $y(j, M)$ to decrease the magnitude of the DFSBC error. This addition is done as

$$y^{k+1}(j, M) = y^k(j, M) + \theta_0 y'(j, M).$$

The use of the SOR method at the free surface greatly speeds up the convergence of the model.

The solution procedure may be summarized as follows. The grid is swept numerous times, using finite difference equation (7). Then the free surface boundary conditions are used iteratively to adjust the free surface shape to best satisfy the fit to the boundary conditions, given the present values of the internal grid points. Then the process is repeated a number of times until convergence is achieved.

APPLICATIONS OF THE MODEL

Uniform Current Case

Before examining in detail waves propagating on currents with arbitrary vorticity, it is helpful to have a means of representing the steady current profile in the absence of waves in the $x-\psi$ plane, both for comparison with the results of the model and for determining input data. For a steady uniform current, all variations with respect to the x direction are zero. Dubreil-Jacotin equation (4) simplifies greatly to

$$y_{\psi\psi} + y_{\psi}^3 f(\psi) = 0. \quad (14)$$

This equation is separable through the use of the substitution $w = y_\psi$ with the results

$$w^{-2} = 2 \int f(\psi) d\psi. \quad (15)$$

The parameter w is equal by definition to $-(U - C)^{-1}$, and, therefore, the above equation may be solved for U ,

$$U(\psi) = C - \left(2 \int_0^\psi f(\psi') d\psi' + C^2 \right)^{1/2}. \quad (16)$$

The value C represents the velocity of the reference frame.

To determine the elevation of the streamline ψ which has the velocity $U(\psi)$, a further integration of (16) is necessary,

$$y(\psi) = \int_0^\psi \left[2 \int_0^\psi f(\psi') d\psi' + C^2 \right]^{-1/2} d\psi. \quad (17)$$

As an example of the use of these equations, for the linear shear current, where the fluid has a constant vorticity, $-\omega_o$, the velocity profile is readily found to be

$$U(\psi) = C - (C^2 - 2\omega_o\psi)^{1/2}. \quad (18)$$

The elevations of the streamlines are expressed as

$$y(\psi) = (1/\omega_o)[C - (C^2 - 2\omega_o\psi)^{1/2}]. \quad (19)$$

To determine the value of the surface streamline, ψ_n , which has the elevation, h , the above equation is used to find

$$\psi_n = Ch - (\omega_o h^2 / 2). \quad (20)$$

Suffice to say, that for more general vorticity distributions, the integrals in Eqs. (16) and (17) can be quite difficult to obtain analytically.

Comparison to Numerical Shear Current Model

A test of the theoretical validity of the finite difference model was conducted by comparing it to the results of the numerical linear shear current model of Dalrymple (7).

The case selected was a wave 2.0 ft in height and a period of 10 seconds propagating in 10 ft of water against a shear current with $\omega_o = -0.30 \text{ sec}^{-1}$. First, a nineteenth-order numerical shear current wave was generated. From this solution, values of kh and ψ_n were obtained for the finite difference model. For starting values of $y(j, i)$, the linear Daubert solution (9), was used to initiate a 30×25 grid. This initial solution had a DFSBC error of 0.01 ft^2 . The finite difference procedure was then used to improve this solution, and after 200 iterations a minimum in the DFSBC error was achieved of $3.97 \times 10^{-5} \text{ ft}^2$. The final results are given in Table I, along with the corresponding results of the numerical shear current theory. For all the parameters of

TABLE I

Comparison of the Linear Shear Current Model and Finite Difference Representations of a Wave Propagating on an Opposing Linear Shear Current for the Same $\psi(x, \eta)$ and kh

Desired Wave Characteristics:

$$H = 2.0 \text{ ft}, T = 10 \text{ sec}, h = 10 \text{ ft}, \omega_0 = -0.3 \text{ sec}^{-1}, \psi_\eta = 178.76 \text{ ft}^2/\text{sec}, kh = 0.3817$$

Model	Dynamic free surface boundary condition error, E_1 (ft ²)	Mean sea level error (ft)	Wave height error (ft)	Wave period, T (sec)
Linear shear current (19th Order)	5.90×10^{-6}	-4.98×10^{-3}	1.14×10^{-3}	10.0
Finite difference (30 × 25 grid)	3.97×10^{-5}	0.0	-4.77×10^{-6}	9.968
Finite difference (30 × 50 grid)	1.52×10^{-5}	-3.04×10^{-5}	-9.54×10^{-6}	9.975

interest, with the exception of the wave period, the finite difference model is as good or better than the analytical theory. It is interesting to note that had the free surface been fixed at the values prescribed by Daubert's solution and the internal grid points allowed to satisfy the full nonlinear governing difference equation, Eq. (7), that the final DFSBC error would have been reduced only to 3.7×10^{-3} ft², a full two orders of magnitude worse than the result given by the full model.

To determine the effect of grid size on the solution, the values of the 30 × 25 grid after 190 iterations were linearly interpolated into a 30 × 50 grid. After 52 iterations over this grid, a minimum in the DFSBC was achieved of 1.52×10^{-5} ft², or a value over 60% lower than that obtained by the 30 × 25 grid and certainly closer to the DFSBC error of the analytical theory of 5.90×10^{-6} ft². The final results obtained with the 30 × 50 grid are shown also in Table I. Again, the largest disparity between the analytical and the finite difference model lies in the wave period where the discrepancy is 0.025 sec for the 30 × 50 grid. This is due to the accuracy of the input variables (three decimal places) and the method by which the wave period, T , is obtained in the finite difference model; that is, averaging $(-(1/y_\psi))(\psi_n/h)$ along the bottom for C and using the formula

$$T = 2\pi/kC. \tag{21}$$

The derivative, y_ψ , is necessarily obtained by forward differences which results in an error $O(\Delta\psi^2)$, which, of course, is reduced rapidly as $\Delta\psi$ becomes smaller. Thus the more detailed the grid, the more accurate is the wave period, as shown in Table I, by comparing the results of the two grids used.

To compare the results of the finite difference models with the analytical theory more directly, the velocity profile under the wave crest is shown in Fig. 3 for all three representations. The equation to determine the dimensional velocity in finite difference form is

$$U(\psi) = C - \frac{\Delta\psi\psi_\eta}{[y(j+1, i) - y(j-1, i)] h} \quad (22)$$

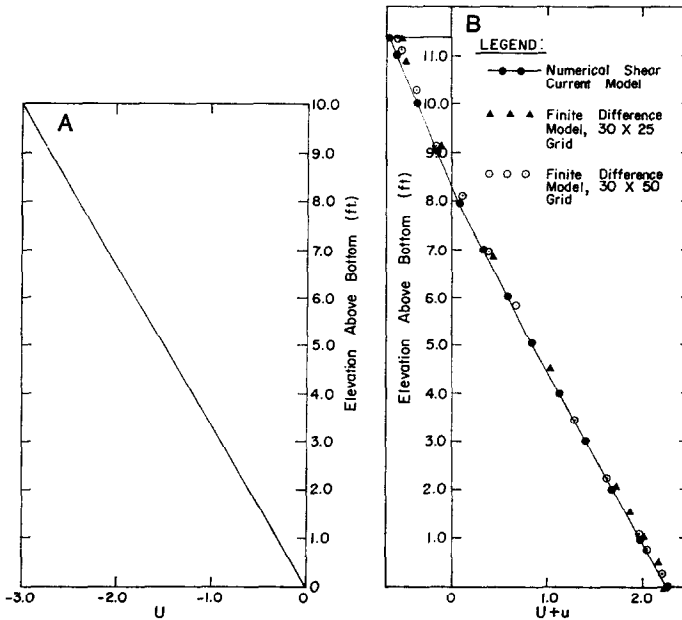


FIG. 3. (a) Linear shear current velocity profile in the absence of a wave. (b) Comparison of horizontal velocity profiles under the wave crest for linear shear current opposing the wave.

Wave characteristics: $H = 2.0$ ft, $T = 10.0$ sec, $h = 10.0$ ft, $\omega_0 = -f(\psi) = -0.3$ sec $^{-1}$, $kh = 0.3817$, $\psi_\eta = 178.76$ ft 2 /sec.

where, again, C is determined by averaging $-(1/y_\psi)(\psi_\eta/h)$ along the bottom streamline, as the wave motion will cancel out.

The agreement between the models is quite good, the most notable difference occurring at the water surface. Also, in Fig. 4, the streamlines under the wave are shown for the analytic model and the 30×50 grid model. The results are in good agreement.

The One-Seventh Power Law

For a wave propagating in an inlet or a river, the ambient current profile is generally logarithmic as a result of turbulence. An approximation to this velocity profile often used is the $(\frac{1}{7})$ power law

$$U = U_{\max}(y/h)^{1/7} \quad (23)$$

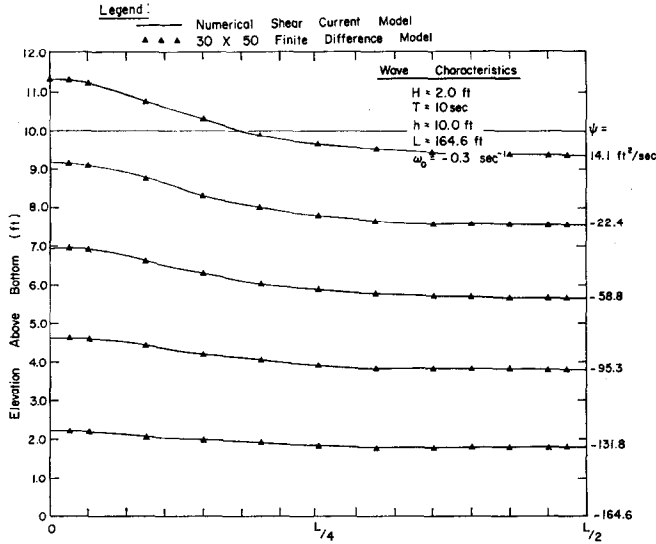


FIG. 4. Comparison of streamline generated by numerical linear shear current model [12] and the finite difference model.

where U_{max} is the maximum velocity, which occurs at the surface and which is taken as -2 fps in this example, h is the water depth, which again is taken as 10 ft. The vorticity of this flow is given as

$$-U_y = -(U_{max}/7h)(y/h)^{-6/7}. \tag{24}$$

In the finite difference model it was assumed that the vorticity varied as

$$f(\psi) = (U_{max}/7h)(y/h)^{-6/7} \tag{25}$$

which does not represent the same current because ψ is not linear in y . However, this vorticity distribution does generate a current profile which is very nearly the same as that of Eq. (24) as can be seen in Fig. 5a, there the differences in velocity at various elevations are less than 0.1 fps. For the wave propagating upstream against the current, a wave height of 2.0 ft was chosen and the kh , ψ_n , and the initial grid values were chosen to be exactly the same as in the previous example. Convergence of the model with a 30×30 grid was achieved in 150 iterations with the minimum DFSBC error of $1.39 \times 10^{-4} \text{ ft}^2$, as shown in Table II, with the other errors. The velocity profile under the wave crest is shown in Figure 5b along with the initially prescribed profile. Recall that the sole difference between these results and those of the previous example (Fig. 3b) is the vorticity distribution as kh , ψ_n , h , and H were taken as the same. The difference in the velocity profile is dramatic.

In Fig. 6, the wave-induced component, u , of the total velocity, $U + u$, (obtained by adding the values in 3a to those in 3b and similarly for Fig. 5), has been shown versus elevation for both the $(\frac{2}{7})$ power law current and the linear shear current. There

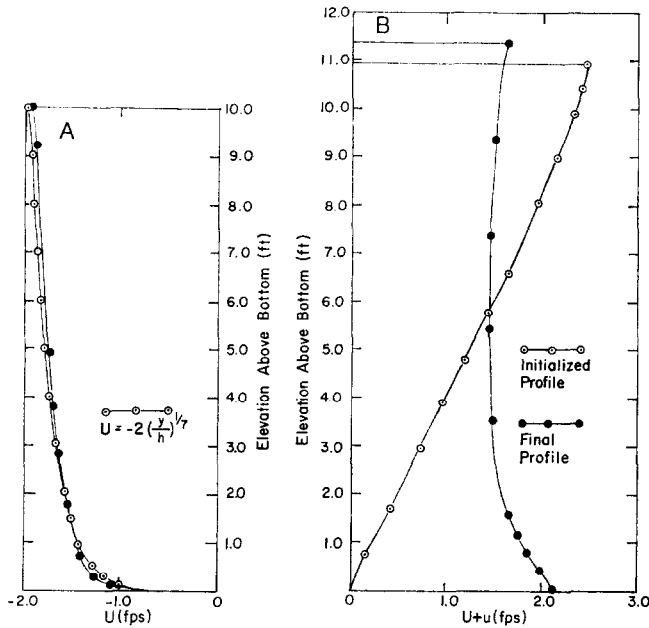


FIG. 5. (a) One-seventh power law current profile in the absence of a wave, based on elevation and stream function. (b) Horizontal velocity profile under the wave crest for one-seventh power law current opposing the wave.

Wave characteristics: $H = 2.0$ ft, $T = 9.49$ sec, $h = 10.0$ ft, $f(\psi) = 0.0285(\psi/\psi_\eta)^{-6/7}$, $kh = 0.3817$, $\psi_\eta = 178.76$ ft²/sec.

TABLE II

Results and Errors in the Finite Difference Representation of a Wave Propagating on an Opposing Turbulent Current

Desired Wave Characteristics:

$$H = 2.0 \text{ ft}, T = 10 \text{ sec}, h = 10 \text{ ft}, f(\psi) = 0.0285(\psi/\psi_\eta)^{-6/7}, \psi_\eta = 178.76 \text{ ft}^2/\text{sec}$$

Model	Dynamic free surface boundary condition error, E_1 (ft ²)	Mean sea level error, (ft)	Wave height error, (ft)	Wave period, T (sec)
Finite difference (30 × 30 grid)	1.39×10^{-4}	-1.84×10^{-5}	-1.67×10^{-5}	9.49

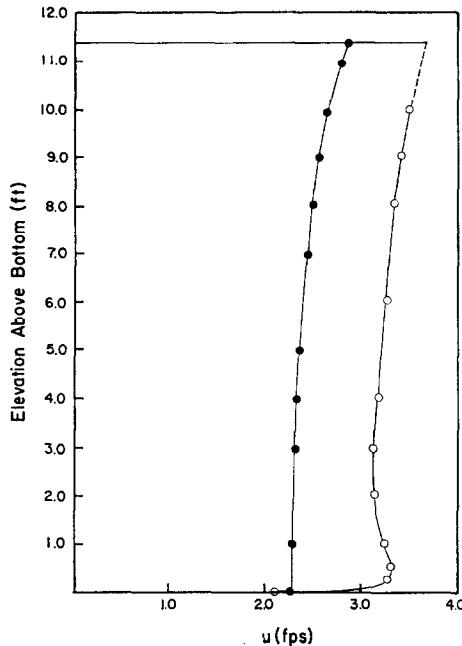


FIG. 6. Wave-induced velocity profiles for the linear shear current and one-seventh power law current under the wave crest. Open circles denote one-seventh power law velocities.

are two noticeable differences between the profiles caused by the different vorticity distributions used: First, the strong vorticity near the bottom for the $(\frac{1}{7})$ power law has induced a forward velocity in the wave-induced motion and second, this same velocity profile is over 30% greater in magnitude than that for the linear shear current. This is primarily due to the fact that the wave period has decreased from 10 to 9.49 sec resulting in a greater wave celerity, C , by Eq. (21), which finally caused greater horizontal velocities, cf. Eqs. (9) and (3). This is a significantly different result than obtained earlier by Dalrymple [21], who showed using a linear shear current that with reasonable accuracy, the water motion under the wave crest could be reasonably well predicted by superimposing the current and the wave velocity profile.

CONCLUSIONS AND FURTHER WORK

A nonlinear finite difference model has been developed for finite amplitude gravity waves on vertically sheared currents. Applications to linear shear and $(\frac{1}{7})$ power law currents show significant differences in horizontal velocity profiles and the importance of vorticity in determining the water particle kinematics under the waves.

Further work is necessary to improve the convergence rate of the model and to allow the model to generate waves on flows which are not colinear with the wave direction. This last change can be instituted quite easily as discussed by Dalrymple [22] to whom the interested reader is referred for more details of the model.

ACKNOWLEDGMENTS

This research has been sponsored, in part, by the following participants of the joint industry project, "Wave Force Analysis and Design Procedure Development," at the University of Florida: Amoco Production Company, Cities Service Oil Company, Chevron Oil Field Research Company, Continental Oil Company, Gulf Research & Development Company, Mobil Research & Development Corporation, Pennzoil United, Incorporated, Phillips Petroleum Company, Placid Oil Company, Shell Oil Company, Texaco Incorporated, Union Oil Company of California. Dr. Frank Hsu of Amoco Production Company has served as Project Manager.

Professor Robert G. Dean aided the author in all stages of this research and his moral encouragement and guidance is greatly appreciated.

REFERENCES

1. G. B. AIRY, Tides and waves in "Encyclopedia Metropolitana," Vol. 5, pp. 241-396, 1845.
2. S. G. STOKES, *Trans. Cambridge Philos. Soc.* **8** (1847), 441-455.
3. L. SKJELBREIA AND J. HENDERSON, Proceedings of the 7th Conference on Coastal Engineering, ASCE, The Hague, 1960.
4. F. GERSTNER, "Abhandlungen der Königlichen Böhmisches Gesellschaft der Wissenschaften," Prague, 1802.
5. J. E. CHAPPELEAR, *J. Geophys. Res.* **66** (1961), 501-508.
6. R. G. DEAN, *J. Geophys. Res.* **75** (1965), 4561-4572.
7. R. A. DALRYMPLE, *J. Geophys. Res.* **79** (1974), 4498-4504.
8. R. A. DALRYMPLE AND J. C. COX, *J. Phys. Ocean.* **6** (1976), 847-852.
9. C. W. HIRT, J. L. COOK, AND T. D. BUTLER, *J. Computational Phys.* **5** (1970), 103-124.
10. B. D. NICHOLS AND C. W. HIRT, *J. Computational Phys.* **12** (1973), 234-246.
11. R. K.-C. CHAN AND R. L. STREET, *J. Computational Phys.* **6** (1970), 68-94.
12. R. K.-C. CHAN, *J. Computational Phys.* **16** (1974), 32-48.
13. J. VON SCHWIND AND R. O. REID, *J. Geophys. Res.* **77** (1972), 420-433.
14. M. L. DUBREIL-JACOTIN, *J. Math.* **13** (1934), 217-291.
15. T. LEVI-CIVITA, *Math. Ann.* **93** (1925), 264-314.
16. D. J. STRUICK, *Math. Ann.* **95** (1926), 595-634.
17. A. DAUBERT, "Publication Scientifiques et Techniques, Du Ministère de l'Air," No. 375, pp. 1-97, 1961.
18. T. BROOKE-BENJAMIN, *J. Fluid Mech.* **12** (1962), 97-116.
19. SIR H. LAMB, "Hydrodynamics," 6th ed., Dover, New York, 1945.
20. P. J. ROACHE, "Computational Fluid Dynamics," Hermosa Publishers, Albuquerque, 1972.
21. R. A. DALRYMPLE, Proc. Offshore Tech. Conf., No. 2114, May 1974.
22. R. A. DALRYMPLE, "Water Wave Models and Wave Forces with Shear Currents," Coastal and Ocean Engng. Lab., Rept. No. 20, Univ. of Fla., p. 163, Gainesville, 1973.